Cross comparison of aeroelastic state-of-the-art design tools on a 10 MW scale wind turbine

D.I. Manolas[1], G.R. Pirrung[2], A. Croce[3], V.A. Riziotis[1], H.A. Madsen[2], S.G. Voutsinas[1], F. Rasmussen[2]

1: School of Mechanical Engineering, National Technical University of Athens
9 Heroon Polytechneiou Str., GR15780, Athens, Greece

2: Wind Energy Department, Technical University of Denmark, Frederiksborgvej 399, Building 118, DK-4000 Roskilde, Denmark

3: Department of Aerospace Science and Technology, Politecnico di Milano, 20156 Milano, Italy

(*) Correspondent author: manolasd@fluid.mech.ntua.gr, tel. +30 2107721097, fax. +30 2107721057

Introduction

The up-scaling of modern turbines towards the 20 MW size, a target set by the wind community [1] in the past years, imposes weight requirements for the blades and calls for improved aerodynamic performance of the rotor with the aim to balance subsequent increase in costs for example of the tower and the underwater support structure. The design of innovative large scale, flexible, low induction rotors that comply with the reduced weights and optimized aerodynamic performance requirements is the main focus of Innwind.eu, Work Package 2. In this framework and with the aim to evaluate the new innovative concepts in terms of specific performance indicators (PI) a number of state-of-the-art aeroelastic design tools have been employed. In the first phase of the project a cross comparison of these tools is performed on a reference 10 MW wind turbine designed by DTU [2].

Approach

Under Work Package 2 of Innwind.eu project the targets of the definition, assessment and demonstration of new innovative lightweight blade and rotor concepts have been set. These new concepts will integrate new aerodynamic and structural design opportunities as well as innovative control strategies for reduced loads and weights. New non-conventional airfoil shapes suitable of low induction rotors, light weight internal structures, passive and active control methods are some of the options investigated in the project. The ultimate goal is to evaluate these design options in terms of specific PIs and qualify the most promising ones for further investigation. In order to evaluate the proposed designs a number of state-of-the-art aeroelastic tools have been employed. From the point of view of the structural analysis, such tools must be able to predict non-linear geometric coupling effects due to large deflections as the proposed designs are expected to be lightweight and therefore very flexible. Also they must be able to account for structural coupling effects due to structural tailoring of the inner structure as for example twist-bending coupling effect. On the other hand, from the point of view of the aerodynamics they must be able to handle new aerodynamic challenges stemming from the up-scaling of the rotor as for example dynamic inflow effects due to 1P excitation which in case of up-scaled rotors becomes more pronounced as the rotational frequency is getting closer to the frequency that the wind spectrum exhibits its maximum energy.

The structural part of the aeroelastic tools employed in the present work is based on Timoshenko beam modelling of the turbine components formulated on a multi-body context [3],[4].[5]. So, by definition the models can handle light-weight flexible structures. As concerns rotor aerodynamics various Blade Element Momentum (BEM) type models are available as well as more advance free wake vortex models [6] or prescribed wake hybrid models [7].

In the first phase of the project structural and aerodynamic load predictions of the abovementioned tools are cross compared on a reference 10 MW wind turbine with the aim to identify possible shortcomings of the applied methodologies mainly in relation to the scale of the turbine analyzed.

Main Body

The cross comparison of the aeroelastic tools consists of the following test cases: (i) comparison of natural frequencies and mode shapes, (ii) comparison of deflections in the case of external static loading and (iii) comparison of loads in normal wind turbine operation with turbulent inflow. The aim of the first two sets is to separately validate the structural models while in the third the full aeroelastic models of the blade and the wind turbine, as a whole, are validated.

Within the framework of the Work Package, 3D Finite Element (F.E.M.) models are also used with the aim to evaluate innovative structural blade designs. Therefore, as part of the package work plan natural frequencies and mode shape predictions from detailed 3D tools have been made available for comparison against beam model predictions. In Table 1 the natural frequencies predictions of three aeroelastic tools (beam models) are compared to 3D F.E.M. predictions obtained with NISA F.E.M. code. The frequencies are listed in order of magnitude from lower to higher values. Overall 3D F.E.M seems to predict slightly higher frequencies of the first five modes. Higher deviations are noted in the predictions of the second flapwise mode (mode 3). The shape of the second flapwise mode is presented in Figure 1(a). It is seen that all beam models underestimate the coupling with the torsion direction predicted by the 3D F.E.M model. Some high deviations are also noted in the frequency of the torsional mode (mode 6). One of the tools identifies the first torsion mode outside of the range of the first eight modes present in the table. It is clear that at least three modes lie in the frequency range of [5-6.5 Hz] which indicates a strong coupling between directions of deflections in these modes. This is depicted in Figure 1(b) where the shape of the third edgewise mode is shown. A strong coupling with the flapwise direction is predicted by all models. Overall the agreement of the beam models with the 3D F.E.M model is fair.

The torsion angle distribution along the blade span resulting from a static load case where a distributed flapwise force of 9 kN has been applied along the blade span is presented in Figure 2. Overall the agreement of the results of the two codes compared in this case is good. The maximum flapwise deflection at the tip of the blade in this static load case (not shown in the plots) is about 10% or the radius. Torsion deformation in this case is partially contributed by bending torsion coupling which is triggered by the very high flapwise deflections and partially by the offset of the shear centre with respect to the elastic axis. The maximum predicted torsion angle at the tip ranges from -1.2^o to -1.4^o. The shape of the deflection is similar in both codes.

Indicative results from purely aerodynamic and full aeroelastic simulations with turbulent wind are presented in Figure 3-Figure 5. Simulations are performed at a mean wind speed 8 m/s while the same turbulent wind input (turbulence intensity of about 20%) has been used in all simulations and by all models. In Figure 3(a) and (b) the Power Spectral Density (PSD) and the rainflow counting plot of the flapwise bending moment at the root of the blade are shown for the case of a purely aerodynamic simulation (stiff wind turbine) in open loop. Different aerodynamic options have been tested in this case including frozen wake simulations (indicated as BEM no dyn in the plots), BEM model enhanced with standard dynamic inflow correction models (indicated as BEM in the plots), hybrid wake models combining a standard BEM implementation for the far wake and a prescribed vortex model for the near wake part (indicated as NW in the plots) and free wake vortex models (indicated as GenUVP in the plots). Comparison of the results shows that, as expected, the frozen wake model significantly overestimates the response of the flapwise moment to the multiples of the rotational frequency and therefore the corresponding load ranges. A relatively high difference is noted between the different implementations of the BEM dynamic inflow models in the different codes while the free wake model lies in between the predictions of the BEM options. The uncertainty of the predictions is definitely linked to the increased azimuthal variation of the rotationally sampled inflow. For larger wind turbines more energy from the turbulent wind spectrum is concentrated to the 1P, 2P etc [8] which imposes challenges to engineering BEM based models. A small difference in the delay effect predicted by the far wake dynamic inflow model and the shed vorticity unsteady aerodynamic model can lead to significantly different dynamic loads results.

In Figure 4 the Power Spectral Density (PSD) of the pitching moment at the root of the blade is shown for the case of a full aeroelastic simulation in closed loop (active controller) at the same wind speed (same turbulent wind as before). Both codes agree well in the 1P peak which dominates the response. One of the codes predicts a peak at ~0.9 Hz which corresponds to the frequency of the first edgewise mode. Cross talking of the torsion with the edgewise direction takes place as a results of the geometric torsion/bending coupling effect which gets more pronounced when high flapwise deflections occur [5]. Again for the case of the full aeroelastic simulation, in Figure 5(a) and (b) the rainflow counting plot of the flapwise bending moment at the root of the blade and tower base fore-aft bending moment at the base of the tower are shown. The agreement between the two codes compared in the plots is good both at the low and the high range cycles.

Conclusions

Simulation results of various state of the art aeroelastic tools are cross compared on a conceptual 10 MW wind turbine. Several structural and aerodynamic effects related to the scale of the turbine under consideration are highlighted and investigated. Overall the level of agreement of the codes is satisfactory. Through the comparison study it was highlighted that some of effects as for example the increased azimuthal variation of the inflow velocity and the blade torsion due to geometric non linearities generate higher levels of uncertainty.

Learning Objectives

- Aerodynamic and structural response of large scale wind turbine
- Investigation of the level of uncertainty of state of the art aeroelastic tools in the prediction of the loads of large scale turbines

References

[1] Sieros, G., Chaviaropoulos, P.K., Sørensen, J.D., Bulder, B.,H., Jamieson, P., 2012, "Up-scaling Wind Turbines: Theoretical and practical aspects and their impact on the cost of energy," J Wind Energy, vol.15, issue 1, pp. 3-17.

[2] Bak, C., Zahle, F., Bitsche, R., Kim, T., Yde, A., Henriksen, L.C., Natarajan, A., Hansen, M.H., "Description of the DTU 10 MW Reference Wind Turbine, " DTU Wind Energy Report-I-0092, 2013.

[3] Larsen T J, Hansen A, Buhl T, Aeroelastic effects of large blade deflections for wind turbines, Proceedings of the special topic conference "The Science of making Torque from Wind" 2004 , pp. 238–246.

[4] Bottasso, C.L., Croce, A., 2006–2015. Cp-Lambda User's Manual. Dipartimento di Scienze e Tecnologie Aerospaziali, Politecnico di Milano, Milano, Italy

[5] Manolas D.I., Riziotis, V.A., Voutsinas, S.G, (2014) "Assessing the importance of geometric non-linear effects in the prediction of wind turbine blade loads", Computational and Nonlinear Dynamics Journal 2014, in press (published on line).

[6] Voutsinas S. G., 2006, "Vortex methods in aeronautics: how to make things work", International Journal of Computational Fluid Dynamics, Vol. 20, pp. 3–18

[7] Pirrung GR H A Madsen, Kim T, Heinz J. "A Coupled Near and Far Wake Model for Wind Turbine Aerodynamics," submitted to Wind Energy, September 2014.

[8] Riziotis, V.A., Madsen, H.A., Rasmussen, F., Politis, E.S., Voutsinas, S.G., (2012), "Implications on loads by up-scaling towards 20MW size," EWEA Annual Event, 16-19 April 2012, Copenhagen.

	Beam models				3D-FEM
	mode	hGAST	Cp-lambda	HAWC2	NISA
1	1st flap	0.62	0.62	0.61	0.64
2	1st edge	0.94	0.94	0.93	0.96
3	2nd flap	1.76	1.76	1.74	1.85
4	2nd edge	2.80	2.80	2.77	2.86
5	3rd flap	3.59	3.60	3.57	3.76
6	1st torsion	5.40	-	6.60	6.01
7	3rd edge	5.73	5.74	5.70	5.82
8	4th flap	6.09	6.11	6.11	

Table 1: Blade natural frequencies. Comparison of predictions of Beam models against 3D FEM models

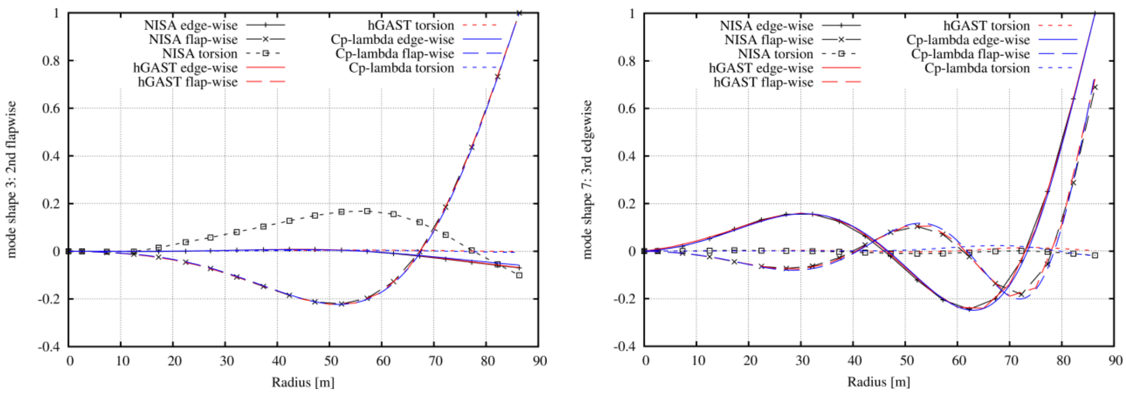

(a) (b)

Figure 1: Comparison of the second flapwise and third edgewise mode against 3D F.E.M, predictions.

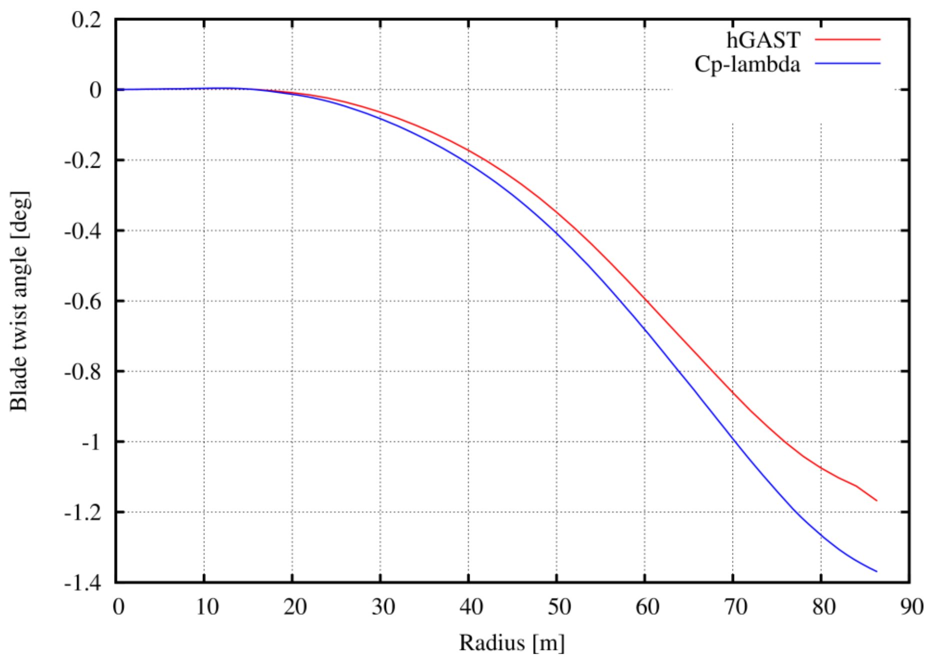

Figure 2: Blade tip torsion angle in the case of a static loading with a distributed flapwise force of 9kN.

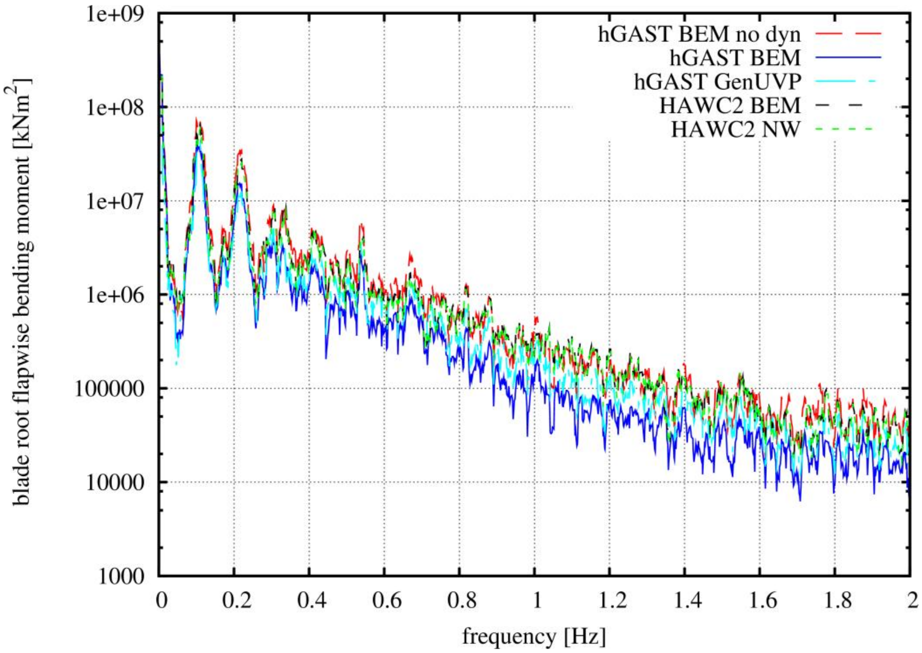

(a)

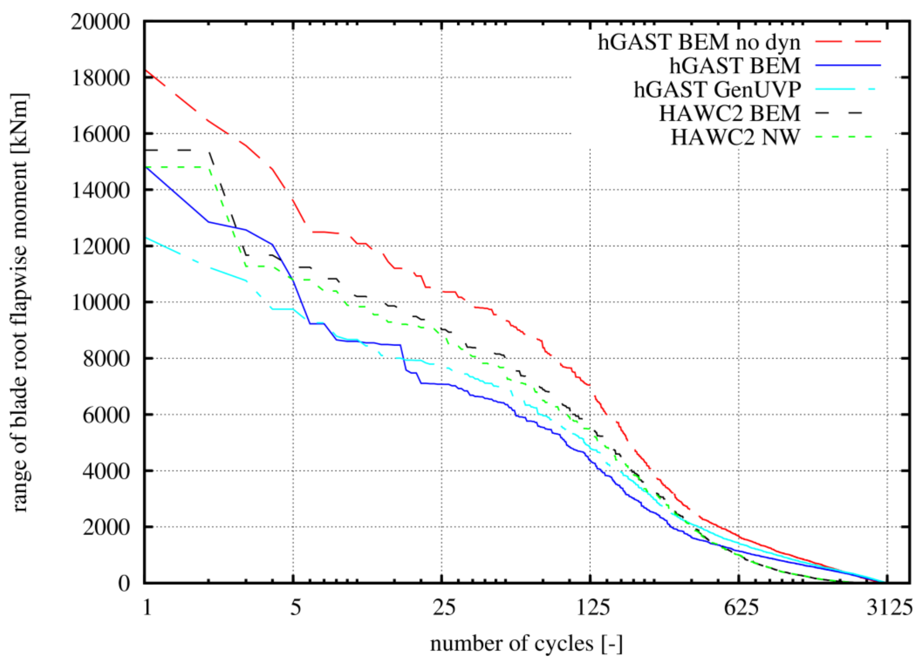

(b)

Figure 3: PSD and rainflow counting plot of flapwise bending moment at the root of the blade for a stiff turbine – normal operation, wind speed 8 m/s.

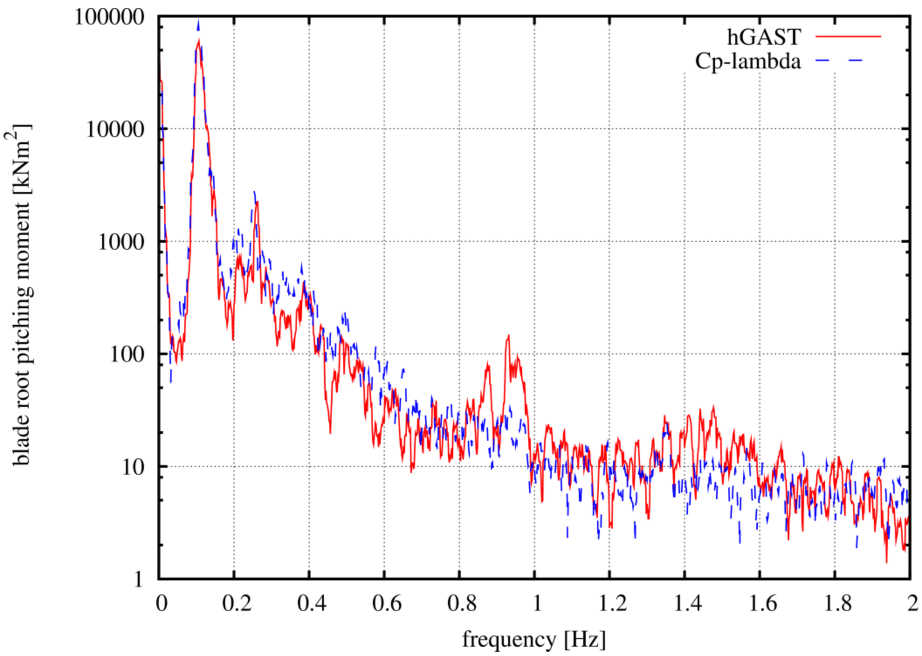

Figure 4: PSD of the blade root pitching moment – normal operation, wind speed 8 m/s.

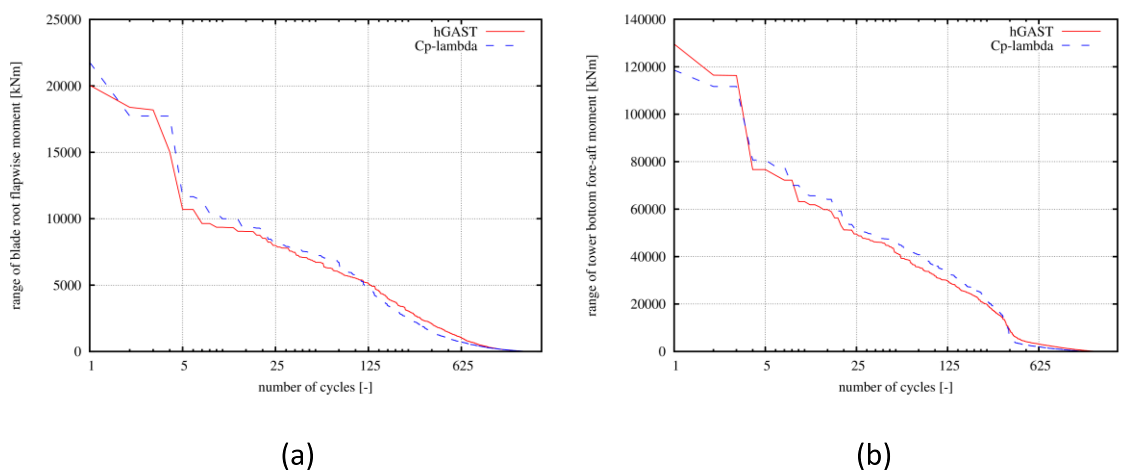

Figure 5: Rainflow counting plot of blade root flapwise bending moment and the tower base fore-aft bending moment – normal operation, wind speed 8 m/s.